

Impact of magnetic field on shear viscosity of quark matter in Nambu-Jona-Lasinio model

Sabyasachi Ghosh¹, Payal Mohanty², Bhaswar Chatterjee³, Arghya Mukharjee⁴, Hiranmaya Mishra⁵

¹ *Indian Institute of Technology Bhilai, GEC Campus, Sejbahar, Raipur-492015, Chhattisgarh, India*

² *National Institute of Science Education and Research, HBNI, 752050 Odisha, India.*

³ *Department of Physics, Indian Institute of Technology Roorkee, Roorkee 247 667, India*

⁴ *Saha Institute of Nuclear Physics, 1/AF Bidhannagar, Kolkata 700064, India and*

⁵ *Theory Division, Physical Research Laboratory, Navrangpura, Ahmedabad 380 009, India*

We have investigated shear viscosity of quark matter in presence of a strong uniform magnetic field background where Nambu-Jona-Lasinio model has been considered to describe the magnetothermodynamical properties of the medium. In presence of magnetic field, shear viscosity coefficient gets split into different components because of anisotropy in tangential stress of the fluid. Four different components can be merged to two components in limit of strong field, where collisional width of quark becomes much lower than its synchrotron frequency. A simplified contact diagram of quark-quark interaction can estimate a small collisional width, where strong field limit expressions are exactly applicable. Although, for RHIC or LHC matter, one can expect a large thermal width, for which generalized four components viscosities are necessary. We have explored these all different possible cases in the thermodynamical framework of Nambu-Jona-Lasinio model.

PACS numbers:

I. INTRODUCTION

One of the major update in the research of heavy ion collision (HIC) experiments like RHIC and LHC is that the produced medium behaves like a nearly perfect fluid [1], with smallest shear viscosity to entropy density ratio (η/s), ever observed in nature. On the other hand, recent progress in the HIC research have speculated that the produced medium may also be subjected to a strong magnetic field [2] in the non-central heavy-ion collisions. The possible space-time dependence of this produced magnetic field has been investigated in Refs. [3–7]. A considerable amount of research work has already been performed in understanding the influence of the magnetic field on the QCD phase diagram. See, for example, the review article [8] for recent updates. The modification of the QCD phase diagram in presence of magnetic field is directly related to the corresponding change in the quark condensate and its enhancement with magnetic field is known as magnetic catalysis (MC) which is quite expected feature in vacuum as well as at finite temperature [9–14]. However, recent calculations, based on lattice quantum chromodynamics (LQCD) [15, 16] have found inverse magnetic catalysis, whose possibility is also indicated by some effective QCD model calculations [17–20]. The modifications pertaining to the QCD phase diagram may also have some impact in the transport properties of the medium produced in HIC. In presence of magnetic field, different transport coefficients like shear viscosity [22–29], bulk viscosity [27–29, 31, 32] and electrical conductivity [33–40] of quark matter are calculated in recent times. The simulation of magnetohydrodynamics [41, 42] as well as the transport simulation for an external magnetic field [43] may require these temperature and magnetic field dependent transport coefficients for their future up-gradation.

Among the different transport coefficients, only the shear viscosity is our matter of interest in the present work, where two flavor Nambu-Jona-Lasinio (NJL) model has been used as a dynamical framework. Among the earlier calculations of shear viscosity for magnetized matter [22–30], we find that Refs. [22–25] have not explored its component decomposition, which is explicitly analyzed in Refs. [26–30]. This component decomposition of shear viscosity due to anisotropy, created by external magnetic field or other sources, is well studied in the direction of gauge gravity duality (See [44, 45] and references therein).

We have first followed the strong field limit expression, obtained in Refs. [26, 49], where four components of shear viscosity merge to two main components, as also found in gauge gravity dual theory [44, 45]. One is normal-type shear viscosity and another is Hall-type component. Normal component depends on both collisional and synchrotron frequencies, but Hall component depends completely on synchrotron frequency in the strong field limit. However, below that strong field limit, both the components can depend on both frequencies. We have also studied on general structure of four different components in the moderate field zone, which is expected in RHIC or LHC experiments.

The article is organized as follows. In Sec. (II), the background formalism of NJL model is addressed. Next Sec.(III) cover the formalism of shear viscosity for the case of strong magnetic field in subsection.(III A) and then its corresponding numerical outcome in subsection.(III B). Realizing strong field limit can not be applicable for RHIC or LHC matter, which should have small collisional relaxation time, we have gone through strong field case to general case, whose modified formalism and corresponding numerical outcome is discussed in Sec. (IV A) and (IV B) respectively. At the end, inves-

tigations of all these different possible cases are summarized in Sec. (V).

II. NJL MODEL IN PRESENCE OF MAGNETIC FIELD

We shall consider here, two flavor (u, d quarks) NJL model with a determinant interaction with the Lagrangian density given as [12, 46]

$$\begin{aligned} \mathcal{L} = & \bar{\psi}(i\not{D} - m)\psi \\ & + G \sum_{a=0}^3 [(\bar{\psi}\tau^a\psi)^2 + (\bar{\psi}i\gamma_5\tau^a\psi)^2] \\ & + K [\det_f \bar{\psi}(1 + \gamma_5)\psi + \det_f \bar{\psi}(1 - \gamma_5)\psi] , \end{aligned} \quad (1)$$

where $\psi = (u, d)^T$ is the doublet of quarks, $m = (m_u, m_d)$ is the current quark mass with $m_u = m_d$. The first term is basically the Dirac Lagrangian in presence of an external magnetic field, which we assume to be constant and in the direction of z -axis. For calculational purpose, we shall further choose the gauge such that the corresponding electromagnetic potential is given by $A_\mu(\mathbf{x}) = (0, 0, Bx, 0)$. The second line is attractive part of the quark anti-quark channel of the Fiertz transformed color current-current interaction. The third line is the 't-Hooft determinant interaction in the flavor space that describes the effects of instantons and is flavor mixing. $\tau^a, a = 0 \dots 3$ are the $U(2)$ generators in the flavor space. In the absence of magnetic field the interaction is invariant under $SU(2)_L \times SU(2)_R \times U_V(1)$. The second term has an additional $U(1)_A$ symmetry while the t-Hooft term does not have this symmetry and reflects the $U(1)_A$ anomaly of QCD.

The thermodynamic potential corresponding to Eq.(1) can be computed exactly in the same manner as was done previously in Ref. [13], that was done for three flavors in a variational method with an explicit structure for the vacuum with quark anti-quark condensates. The thermodynamic potential is then given as

$$\begin{aligned} \Omega = & \sum_i \Omega_0^i + \sum_i \Omega_{field}^i + \sum_i \Omega_{med}^i \\ & + 2G \sum_i I_s^i{}^2 + 2K I_s^u I_s^d \end{aligned} \quad (2)$$

where, i is the flavor index. We might mention here that the above thermodynamic potential can also be derived in a mean field approximation [46]. The vacuum term for i -th flavor Ω_0^i is given as

$$\begin{aligned} \Omega_0^i = & -\frac{2N_c}{(2\pi)^3} \int d\mathbf{p} \sqrt{\mathbf{p}^2 + M_i^2} \theta(\Lambda - |\mathbf{p}|) \\ = & -\frac{N_c}{8\pi^2} \left[\Lambda \sqrt{\Lambda^2 + M_i^2} (2\Lambda^2 + M_i^2) \right. \\ & \left. - M_i^4 \log \frac{\Lambda + \sqrt{\Lambda^2 + M_i^2}}{M_i} \right], \end{aligned} \quad (3)$$

with, Λ as the three momentum cutoff associated with the NJL model. The field contribution that arises from the effect of magnetic field on the Dirac vacuum is given by

$$\begin{aligned} \Omega_{field}^i = & -\frac{N_c}{2\pi^2} \sum_i |q_i B|^2 \left[\zeta'(-1, x_i) \right. \\ & \left. - \frac{1}{2}(x_i^2 - x_i) \ln x_i + \frac{x_i^2}{4} \right], \end{aligned} \quad (4)$$

where we have defined a dimension less quantity, $x_i = M_i^2/2|q_i B|$, i.e. the mass parameter in units of magnetic field and $\zeta'(-1, x) = d\zeta(z, x)/dz|_{z=-1}$ is the derivative of the Riemann-Hurwitz ζ function which is given by

$$\begin{aligned} \zeta'(-1, x) = & \frac{\ln x}{2} \left[x^2 - x + \frac{1}{6} \right] - \frac{x^2}{4} \\ & + x^2 \int_0^\infty \frac{2 \tan^{-1} y + y \ln(1 + y^2)}{e^{2\pi x y} - 1} dy. \end{aligned} \quad (5)$$

Finally, the medium contribution Ω_{med}^i is given as

$$\Omega_{med}^i = \frac{-N_c}{\pi^2} \sum_{n=0}^{n_{max}} \frac{\alpha_n |q_i B|}{\beta} \int dp_z \log(1 + e^{-\beta \omega_n^i}) \quad (6)$$

with the single particle energy in presence of magnetic field $\omega_n^i = \sqrt{p_z^2 + 2n|q_i B| + m^2}$. The condition of a sharp three momentum cutoff translates to a finite number of Landau level summation with $n_{max} = \text{Int}[\frac{\Lambda^2}{2|q_i B|}]$ when $p_z = 0$. Further, for the medium contributions this also leads to a cutoff for the $|p_z|$ as $\Lambda' = \sqrt{\Lambda^2 - 2n|q_i B|}$ for a given value of n .

Similarly, in Eq.(2), the quark condensate $I_s^i = -\langle \bar{\psi}^i \psi^i \rangle$, can be separated into a zero field vacuum term, a finite field dependent term and a medium dependent term as

$$\begin{aligned} I_s^i \equiv & -\langle \bar{\psi}^i \psi^i \rangle = \frac{2N_c}{(2\pi)^3} \int_{|\mathbf{p}| < \Lambda} d\mathbf{p} \frac{M^i}{\sqrt{\mathbf{p}^2 + M^i{}^2}} \\ & + \frac{N_c M^i |q^i B|}{(2\pi)^2} [x^i (1 - \ln x^i) \\ & \quad + \ln \Gamma(x^i) + \frac{1}{2} \ln \frac{x^i}{2\pi}] \\ & - \sum_{n=0}^{n_{max}} \frac{N_c |q^i B| \alpha_n}{(2\pi)^2} \int dp_z \frac{M^i}{\omega_n^i} \frac{1}{1 + e^{-\beta \omega_n^i}} \\ = & I_{svac}^i + I_{sfield}^i + I_{smed}^i. \end{aligned} \quad (7)$$

The zero field vacuum contribution, I_{svac}^i , can be analytically calculated using a sharp momentum cutoff Λ and can be written as

$$\begin{aligned} I_{svac}^i = & \frac{N_c M_s^i}{2\pi^2} \left[\Lambda \sqrt{\Lambda^2 + M^i{}^2} \right. \\ & \left. - M^i{}^2 \log \left\{ \frac{\Lambda + \sqrt{\Lambda^2 + M^i{}^2}}{M^i} \right\} \right]. \end{aligned} \quad (8)$$

The constituent quark mass M^i satisfies the gap equation

$$M_i = m_i + 4GI_s^i + 2K|\epsilon^{ij}|J_s^j. \quad (9)$$

This completes the definitions of all the quantities which are used to describe the thermodynamic potential in Eq.(2).

For numerical evaluations we choose the parameters as in Ref.[46] i.e. we write $G = (1 - \alpha)G_0$ and $K/2 = \alpha G_0$. The parameter α controls the strength of the instanton interaction while the value of the quark condensate is determined by the combination of parameters : $m = 6$ MeV, the three momentum cut off $\Lambda = 590$ MeV and the dimensionless coupling $G_0\Lambda^2 = 2.435$. These values lead to pion mass in vacuum as 140.2 MeV, pion decay constant of 92.6 MeV and quark condensate $\langle \bar{u}u \rangle = \langle \bar{d}d \rangle = (-241.5 \text{ MeV})^3$, all in reasonable agreement with the experimental values. This also leads to a vacuum constituent quark mass of 400 MeV. Further, in all these calculations we have taken $\alpha = 0.15$ as a reasonable value interpolated from $\eta - \eta'$ splitting within 3-flavor NJL model [46].

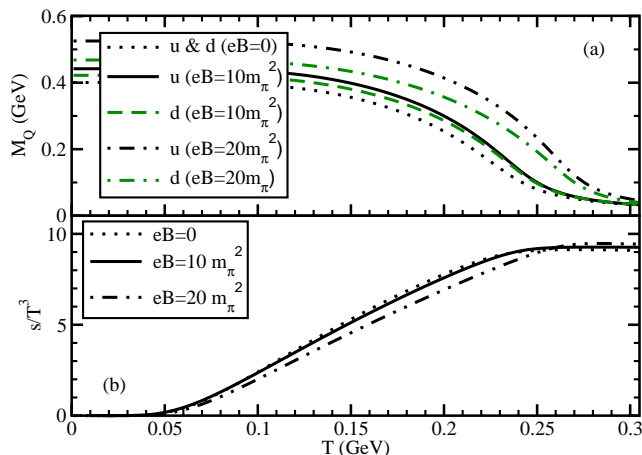


FIG. 1: T dependence of constituent quark masses (M_Q) and normalized entropy density (s/T^3) for different values of magnetic fields.

Fig. 1(a) shows the constituent quark mass as a function of temperature for different values of magnetic fields. At $eB = 0$, masses of u and d quarks exactly coincide (dotted line), while for non-zero eB , they split due to different electrical charges of the two quark flavors and their splitting increases with the magnetic field. Our results reveal the magnetic catalysis in entire temperature range and therefore, transition temperature T_c increases with B . Using this $M_Q(T, eB)$, one can calculate entropy density s with the help of a quasi-particle relation:

$$s = \frac{N_c}{\pi^2 T} \sum_{i=u,d} \sum_{n=0}^{n_{\max}} \alpha_n |q_i| B \int d\mathbf{k}_z \left[\frac{\mathbf{k}_z^2}{\omega_n^i} + \omega_n^i \right] f_0(\omega_n^i), \quad (10)$$

where $f_0(\omega_n^i)$ is Fermi-Dirac distribution function. The temperature dependence of normalized entropy density s/T^3 for $eB = 0$ (dotted line), $10m_\pi^2$ (solid line) and $20m_\pi^2$ (dash-dotted line) are shown in Fig. 1(b). We notice that s decreases as eB increases in lower temperature domain but all the curves are merged into its Stefan-Boltzmann (SB) limit at high temperature region.

III. STRONG MAGNETIC FIELD CASE

A. Formalism of shear viscosity in presence of strong magnetic field

Let us first take a brief recapitulation of relaxation time approximation (RTA) technique to calculate shear viscosity coefficients of a relativistic fluid in absence of any magnetic field (i.e. $B = 0$), which is elaborately given in Refs. [47, 48]. Then, we will come to its corresponding formalism in presence of the **strong** magnetic field, well described in Refs. [26, 49].

Total energy-momentum tensor of relativistic fluid, $T^{\mu\nu} = T_0^{\mu\nu} + T_D^{\mu\nu}$ contains ideal part $T_0^{\mu\nu} = -Pg^{\mu\nu} + (P + \epsilon)u^\mu u^\nu$ and dissipation part $T_D^{\mu\nu} = \eta U^{\mu\nu}$ (only shear dissipation), where P , ϵ , u^μ are respectively pressure, energy density and four velocity of the fluid. The tensor structure $U^{\mu\nu}$, linked with shear viscosity η , has a form [48]:

$$U^{\mu\nu} = D^\mu u^\nu + D^\nu u^\mu + \frac{2}{3} \Delta^{\mu\nu} \partial_\sigma u^\sigma \quad \text{with} \\ D^\mu = \partial^\mu - u^\mu u^\sigma \partial_\sigma, \quad \Delta^{\mu\nu} = u^\mu u^\nu - g^{\mu\nu}. \quad (11)$$

Now, in terms of four momentum $k^\mu = (\omega, \mathbf{k})$ and thermal distribution function $f_0 = 1/\{e^{\beta\omega} + 1\}$ of quark at temperature $T = 1/\beta$, one can express the total energy-momentum tensor as

$$T^{\mu\nu} = \int \frac{d^3 \mathbf{k}}{(2\pi)^3} \frac{k^\mu k^\nu}{\omega} \{f_0 + \phi f_0(1 - f_0)\}, \quad (12)$$

where, the second term in the curly bracket involving the function ϕ describes the non-equilibrium part for which one can construct the shear dissipative part $T_D^{\mu\nu}$ of the energy momentum tensor [48]. In terms of velocity gradient tensor $U^{\mu\nu}$, the function ϕ can be written as $\phi = C k_\mu k_\nu U^{\mu\nu}$. The unknown C can be obtained as $C = \frac{\tau_c \beta}{2\omega}$ by using the relativistic Boltzmann equation (RBE), where τ_c is the relaxation time of the quark in the medium. Comparing the coefficients of $U^{\mu\nu}$ from the dissipative part of the energy-momentum tensor, we finally obtain the expression of shear viscosity coefficient as

$$\eta = \frac{g\beta}{15} \int \frac{d^3 \mathbf{k}}{(2\pi)^3} \frac{\mathbf{k}^4}{\omega^2} \tau_c f_0(1 - f_0), \quad (13)$$

where $g = 2 \times 2 \times 2 \times 3$ is an additional input that takes care of the degeneracy factor for 2 flavor (isospin symmetric) quark matter.

Now, let us discuss the shear viscosity of the medium in presence of external magnetic field, which is decomposed into five independent components. Therefore, the dissipative part of energy-momentum tensor (in three vector notation) is written as

Now, let us discuss the effect of external magnetic field on the shear viscosity of the medium. In presence of a constant background magnetic field, the medium can possess five independent components of shear viscosity and the dissipative part of the energy-momentum tensor (in three vector notation) can be written as [26, 49]

$$T_D^{ij} = \sum_{n=0}^4 \eta_n V_n^{ij} = \int \frac{d^3 \mathbf{k}}{(2\pi)^3} \frac{k^i k^j}{\omega} \delta f, \quad (14)$$

where

$$\delta f = \phi f_0(1 - f_0) = \sum_{n=0}^4 C_n k^i k^j V_n^{ij} f_0(1 - f_0) \quad (15)$$

and

$$\phi = \sum_{n=0}^4 C_n k^i k^j V_n^{ij} \quad (16)$$

is assumed in terms of same tensorial components V_n^{ij} .

Among these 5 components, 4 components ($n = 1, \dots, 4$) will be our matter of interest as only these components depend on magnetic field, while $n = 0$ component remain unaffected by magnetic field. This $n = 0$ viscosity component can be compared with the electrical/thermal conductivity along the direction of magnetic field, as discussed Refs. [36, 49], where they also remain undisturbed by the external magnetic field. Hence, ignoring the η_0 or V_0^{ij} component [26, 49], one can obtain four shear viscosity coefficients as

$$\eta_{(n=1,2,3,4)}^i = \frac{2g_i}{15} \int \frac{d^3 \mathbf{k}}{(2\pi)^3} \frac{\mathbf{k}^4}{\omega^i} C_{(n=1,2,3,4)}^i f_0^i(1 - f_0^i), \quad (17)$$

where the unknown C_n^i again will be determined with the help of the RBE but in two step approximations. Since the magnetic field will destroy the degeneracy of u and d quark masses, therefore, energy ω^i , distribution function f_0^i and C_n^i in Eq. (17) carry the flavor index i . The $g_i = 2 \times 2 \times 3$ is degeneracy factor of each flavor.

As a first approximation, the particle relaxation time τ_c in the RBE is ignored by assuming that the deviation from equilibrium due to the strong magnetic field is much larger than that due to the particle collisions. Therefore, we get a magnetic field induced relaxation time $\tau_B^i = 1/\omega_B^i$, where

$$\omega_B^i = q_i B / \omega^i, \quad (q_i = +\frac{2}{3}e, -\frac{1}{3}e \text{ for } i = u, d) \quad (18)$$

is the synchrotron frequency of quark. So the strong field limit will be established if we can show that $\tau_c^i \gg \tau_B^i$.

As a first approximation of RBE [26, 49], we ignore τ_c^i leading to the coefficients C^i getting related to the field induced relaxation time τ_B as

$$C_1^i = C_2^i = 0, \text{ and } C_4^i = 2C_3^i = \frac{\tau_B^i \beta}{2\omega^i}. \quad (19)$$

Now, in a second approximation, a collisional or thermal width $\Gamma_c^i = 1/\tau_c^i$, obeying the inequality $\Gamma_c^i \ll \omega_B^i$ or $\tau_c^i \gg \tau_B^i$, is considered which leads to the relation [26]:

$$C_2^i = 4C_1^i = \frac{\Gamma_c^i}{\omega_B^i} C_4^i = \frac{\Gamma_c^i}{2\omega_B^i} C_3^i, \quad (20)$$

with $C_4^i = 2C_3^i = \frac{\tau_B^i \beta}{2\omega^i}$. Thus, in presence of constant background magnetic field B , the expressions of the four components of the shear viscosity for $i = u/d$ quark are

$$\eta_2^i = 4\eta_1^i = \frac{g_i \beta}{15} \int \frac{d^3 \mathbf{k}}{(2\pi)^3} [f_0^i \{1 - f_0^i\}] \left\{ \left(\frac{\Gamma_c^i}{\omega_B^i} \right) \left(\frac{1}{\omega_B^i} \right) \right\} \left(\frac{\mathbf{k}^2}{\omega^i} \right)^2, \quad (21)$$

and

$$\eta_4^i = 2\eta_3^i = \frac{g_i \beta}{15} \int \frac{d^3 \mathbf{k}}{(2\pi)^3} [f_0^i \{1 - f_0^i\}] \left\{ \frac{1}{\omega_B^i} \right\} \left(\frac{\mathbf{k}^2}{\omega^i} \right)^2. \quad (22)$$

If we compare Eqs. (21), (22) with Eq. (13), then we can get a physical interpretation of these shear viscosity components. In the perpendicular plane to the external magnetic field, the momentum transfer due to shear stress is independent of the particle collisions and will be proportional to the field induced relaxation ($\tau_B = 1/\omega_B$) which is basically the inverse of the synchrotron frequency. In other words, rotational motion of the charged particles with corresponding synchrotron frequency provides the required momentum transfer for generating shear stress along the tangential directions, located in the perpendicular plane with respect to the magnetic field. This strength of shear stress, velocity gradient and its proportional coefficients η_3, η_4 are completely originated due to (strong) magnetic field background.

In other possible tangential directions, both the collisional and rotational energies take part in momentum transfer. Therefore, the fraction Γ_c/ω_B is required for fixing the proportional strength of viscosities η_1 and η_2 . The corresponding relaxation time for these components becomes $\left[\left(\frac{\Gamma_c}{\omega_B} \right) \frac{1}{\omega_B} \right]^{-1}$.

B. Results of strong field case

For the strong field limit to be valid τ_c should be much largerr than $\tau_B = 1/\omega_B = \omega_Q^k/eQB = \{\mathbf{k}^2 +$

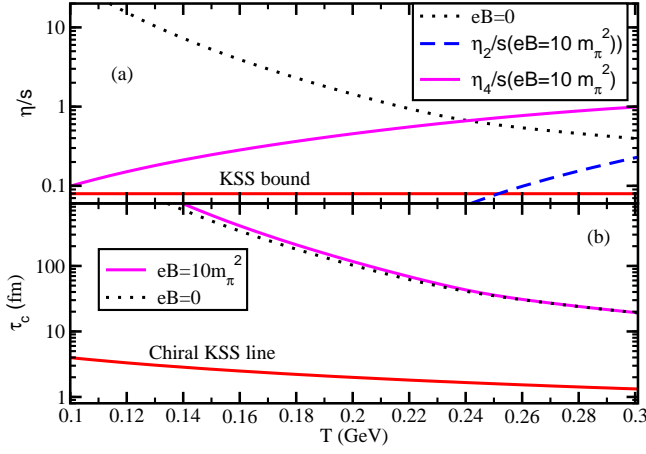


FIG. 2: (a) T dependence of η/s at $eB = 0$ (dotted line) and η_2/s (blue dash line), η_4/s (pink solid line) at $eB = 10m_\pi^2$. (b) T dependence of τ_c at $eB = 0$ (dotted line) and $eB = 10m_\pi^2$ (pink solid line).

$m_Q^2\}^{1/2}/eQB$ [26], which is the inverse of the synchrotron frequency ω_B . The assumption $\tau_c \gg \tau_B$ is the basis of strong field case formalism, discussed in earlier Sec. (III A). After calculating τ_c microscopically, one will be able to know whether the value of τ_c satisfy $\tau_c \gg \tau_B$ or strong field limit or not. Here, we will attempt to obtain $\tau_c(T, eB)$ in a microscopic calculation. For this purpose, let us start with $B = 0$ case with standard expression of collisional relaxation time τ_c or thermal width,

$$\begin{aligned} \Gamma_c(T, \mathbf{k}_a) &= \frac{1}{\tau_c} \\ &= \sum_b \int \frac{d^3k_b}{(2\pi)^3} \sigma_{ab}(T, \mathbf{k}_a, \mathbf{k}_b) v_{ab}(T, \mathbf{k}_a, \mathbf{k}_b) f_b(T, \mathbf{k}_b), \end{aligned} \quad (23)$$

where

$$v_{ab}(T, \mathbf{k}_a, \mathbf{k}_b) = \frac{\{(\omega_a + \omega_b)^2 - 4M_Q^2(T)\}^{1/2}(\omega_a + \omega_b)}{2\omega_a\omega_b} \quad (24)$$

is relative velocity with $\omega_{a,b} = \{\mathbf{k}_{a,b}^2 + M_Q^2(T)\}^{1/2}$. To map grossly the scattering strength of NJL dynamics, let us calculate cross section σ_{ab} from simple four quark contact diagram, shown inside Fig. 2(b). To do it, we use the standard quantum field theoretical relation of $2 \rightarrow 2$ scattering,

$$\sigma_{ab} = \frac{1}{16\pi s} \overline{|M|_{ab}^2}, \quad (25)$$

where $s = (\omega_a + \omega_b)^2$ and

$$\begin{aligned} \overline{|M|_{ab}^2} &= \frac{1}{2 \times 2} G^2 16 \left(\frac{s}{2}\right)^2 \\ &= G^2 s^2, \quad s = (\omega_a + \omega_b)^2. \end{aligned} \quad (26)$$

Hence, we get a temperature and momentum dependence cross section $\sigma_{ab}(T, \mathbf{k}_a, \mathbf{k}_b) = \frac{G^2}{16\pi} s(T, \mathbf{k}_a, \mathbf{k}_b)$.

By maintaining electric charge conservation, we will get 12 possible $2 \rightarrow 2$ ($ab \rightarrow a'b'$) scattering processes :

$$\begin{aligned} u\bar{u} &\rightarrow u\bar{u}, \quad u\bar{d} \rightarrow u\bar{d}, \quad u\bar{u} \rightarrow d\bar{d}, \quad uu \rightarrow uu, \\ ud &\rightarrow ud, \quad \bar{u}\bar{u} \rightarrow \bar{u}\bar{u}, \quad \bar{u}\bar{d} \rightarrow \bar{u}\bar{d}, \quad d\bar{d} \rightarrow d\bar{d}, \\ d\bar{d} &\rightarrow u\bar{u}, \quad d\bar{u} \rightarrow d\bar{u}, \quad dd \rightarrow dd, \quad \bar{d}\bar{d} \rightarrow \bar{d}\bar{d}, \end{aligned} \quad (27)$$

So fixing any initial particle a as probe particle, we have to take summation of b to calculate $\Gamma_c(T, \mathbf{k}_a)$. Taking momentum average of probe particle, we get only T dependent quark width,

$$\begin{aligned} \Gamma_c(T) &= \frac{1}{\tau_c} \\ &= \frac{\int \frac{d^3k_a}{(2\pi)^3} \Gamma(T, \mathbf{k}_a) f_a(T, \mathbf{k}_a)}{\int \frac{d^3k_a}{(2\pi)^3} f_a(T, \mathbf{k}_a)}. \end{aligned} \quad (28)$$

So we find that temperature dependent mainly coming from thermodynamical phase space and $M_Q(T)$. If we go for simplified extension of finite magnetic field picture by replacing $M_Q(T, eB)$ in Eq. (28), we can get $\Gamma_c(T, eB)$. Fig. 2(b) shows the $\tau_c(T, eB)$ at $eB = 0$ (black dotted line), $eB = 10m_\pi^2$ (pink solid line).

Due to increase in the number density of the particles in the medium with temperature, the collisional frequency increases and relaxation time decreases with T . The eB dependence of τ_c enters via eB dependence of constituent quark mass $M_Q(eB)$. Increasing function $M_Q(eB)$ can suppress the number density, which make Γ_c decrease and τ_c increase with eB . Being proportional to the decreasing function $\tau_c(T)$ for $eB = 0$, η/s decreases with T .

Let us note that in the behaviour of η/s with temperature arises from two competing quantities that depend upon temperature. Due to thermodynamic phase space factor, this ratio is an increasing function of temperature while the relaxation time decrease with temperature. For constant relaxation time, due to thermal phase space factor, η/s increase with temperature. This can be easily found out for mass less ideal gas behaviour of the expression for η/s . On the otherhand, for the decreasing behaviour of temperature dependent τ , dominates over the increasing behaviour arising from the thermal phase space making the ratio decreasing with temperature, as may be noticed in dotted line of Fig. 2(a).

Another noticeable thing is that for contact diagram of $2 \rightarrow 2$ scattering processes, NJL model estimate is rather large for τ_c , which is quite far from chiral KSS line $\tau_c(T) = \frac{5}{4\pi T}$, shown by red solid line in Fig. 2(b). The chiral KSS line comes from the demand of $\frac{\eta}{s} = \frac{1}{4\pi}$ for massless particle. Therefore, in Fig. 2(a), black dotted line is also quite far from red horizontal line, denoted KSS value $\frac{\eta}{s} = \frac{1}{4\pi}$.

For this high value of τ_c , $eB = 10m_\pi^2$ can be considered as strong field limit case because τ_B remain within the

range 0.8-3 fm. So we can safely say that at $eB = 10m_\pi^2$, we can consider $\tau_c \gg \tau_B$ or strong field limit case [26]. It is interesting to notice in Eqs. (21) that the position of τ_c for strong field case becomes inverse ($\eta_2 \propto 1/\tau_c$), therefore, η_2/s becomes an increasing function of T , as shown by pink solid line in Fig. 2(a). Hence, in strong field limit, $\eta_{1,2} \propto 1/\tau_c$ follow opposite trend with respect without field case $\eta \propto \tau_c$. When we come to the Hall-type viscosity $\eta_{3,4} \propto \tau_B$, which is appeared as dissipation-free completely as it becomes independent of τ_c . $\eta_{3,4}$ increases with T because of its phase space part, which can be realized from η_4/s curve (blue dash line) in Fig. 2(a).

Now, for simplest contact diagram calculation, we are getting very large value of τ_c but it can not be expected in RHIC or LHC matter, whose life time is approximately 10 fm. So, the strong field case can't be applicable for RHIC or LHC matter, whose τ_c is expected to be small, at least smaller than 10 fm. We might find alternative possible diagrams, which can provide small τ_c . Refs. [50–54] have obtained very small τ_c , relevant to RHIC or LHC matter through meson exchange type diagram, whose calculation in presence of magnetic field is not at all very straight forward. It might be considered as future challenging topics. Instead of calculating smaller $\tau_c(T)$, we can take it as parameter and examine the impact of its smaller value. When we consider small value of τ_c (< 10 fm) at $eB = 10m_\pi^2$, the inequality $\tau_c \gg \tau_B$ does not hold. So instead of considering strong field limit, we might have to find some general structure of η_n , which has been attempted in next section.

IV. FROM STRONG FIELD TO MODERATE FIELDS

A. Modified formalism of shear viscosity

In this section, we will attempt to find a guess general structure of shear viscosities, which can be applicable for any value of τ_B and τ_c .

We have found that the τ_c in Eq. (13) for $B = 0$ is basically replaced by effective relaxation time $\tau_{1,2}^{\text{eff}} = \frac{\tau_B^2}{\tau_c}$ for $\eta_{1,2}$ and $\tau_{3,4}^{\text{eff}} = \tau_B$ for $\eta_{3,4}$. Let us guess an ansatz of effective relaxations:

$$\begin{aligned}\tau_1^{\text{eff}} &= \tau_c \frac{1}{4\{\frac{1}{4} + (\tau_c/\tau_B)^2\}} \\ \tau_2^{\text{eff}} &= \tau_c \frac{1}{\{1 + (\tau_c/\tau_B)^2\}} \\ \tau_3^{\text{eff}} &= \tau_c \frac{\tau_c/\tau_B}{2\{\frac{1}{4} + (\tau_c/\tau_B)^2\}} \\ \tau_4^{\text{eff}} &= \tau_c \frac{\tau_c/\tau_B}{\{1 + (\tau_c/\tau_B)^2\}}\end{aligned}\quad (29)$$

which might be consider as their general structure, be-

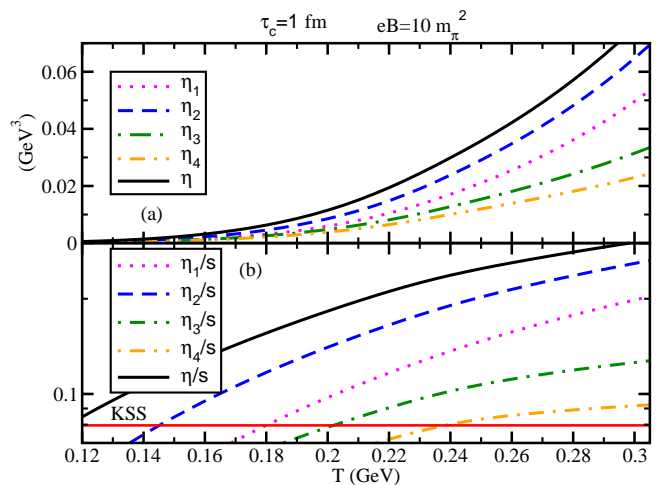


FIG. 3: (a) T dependence of η at $eB = 0$ (solid line) and $\eta_{1,2,3,4}$ (dotted, dash, dash-dotted, dash-double-dotted lines) at $eB = 10m_\pi^2$. (b) Corresponding viscosity to entropy density ratios.

cause in the limit of $\tau_c \gg \tau_B$, we get

$$\begin{aligned}4\tau_1^{\text{eff}} &= \tau_2^{\text{eff}} = \frac{\tau_B^2}{\tau_c} \\ 2\tau_3^{\text{eff}} &= \tau_4^{\text{eff}} = \tau_B.\end{aligned}\quad (30)$$

It means that we will get back Eqs. (21) and (22) for the strong field limit ($\tau_c \gg \tau_B$).

Using that general structure of relaxation (29) in Eqs. (21) and (22) we will get general expressions of shear viscosity components:

$$\eta_1 = \frac{g\beta}{15} \int \frac{d^3\mathbf{k}}{(2\pi)^3} \left(\frac{\mathbf{k}^2}{\omega}\right)^2 \tau_c \frac{1}{4\{\frac{1}{4} + (\tau_c/\tau_B)^2\}} [f_0\{1 - f_0\}] \quad (31)$$

$$\eta_2 = \frac{g\beta}{15} \int \frac{d^3\mathbf{k}}{(2\pi)^3} \left(\frac{\mathbf{k}^2}{\omega}\right)^2 \tau_c \frac{1}{1 + (\tau_c/\tau_B)^2} [f_0\{1 - f_0\}] \quad (32)$$

$$\eta_3 = \frac{g\beta}{15} \int \frac{d^3\mathbf{k}}{(2\pi)^3} \left(\frac{\mathbf{k}^2}{\omega}\right)^2 \tau_c \frac{\tau_c/\tau_B}{2\{\frac{1}{4} + (\tau_c/\tau_B)^2\}} [f_0\{1 - f_0\}] \quad (33)$$

$$\eta_4 = \frac{g\beta}{15} \int \frac{d^3\mathbf{k}}{(2\pi)^3} \left(\frac{\mathbf{k}^2}{\omega}\right)^2 \tau_c \frac{\tau_c/\tau_B}{1 + (\tau_c/\tau_B)^2} [f_0\{1 - f_0\}] \quad (34)$$

B. Modified results for moderate fields

Using Eqs. (31), (32), (33), (34), we have first plotted $\eta_{1,2,3,4}$ vs T in Fig. 3(a) and then their normalized values $\eta_{1,2,3,4}/s$ in Fig. 3(b). Interesting point is that all components of shear viscosity in presence of magnetic field

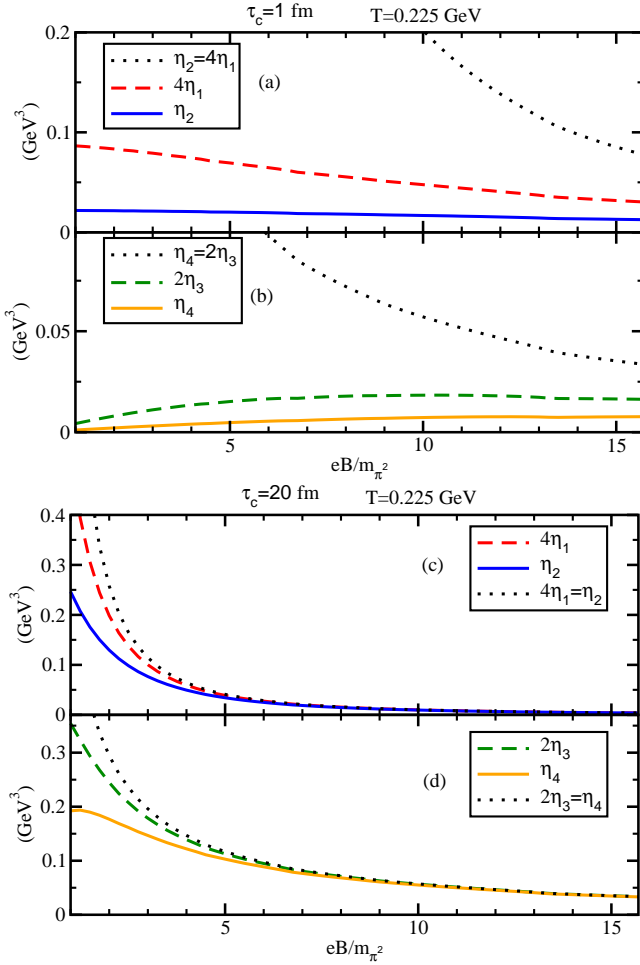


FIG. 4: For $\tau_c = 1$ fm, (a) $4\eta_1$, η_2 from Eqs. (31), (32) respectively and its strong field limit (where $4\eta_1 = \eta_2$) from Eq. (21). Similarly, for $\tau_c = 1$ fm, (b) $2\eta_3$, η_4 from Eqs. (33), (34) respectively and its strong field limit (where $2\eta_3 = \eta_4$) from Eq. (22). (c) and (d) are same as (a) and (b) for $\tau_c = 20$ fm.

is smaller than its isotropic value in absence of magnetic field. In Fig. 3(b), we notice that KSS line is crossing different curves at different temperature. Here, we find that at fixed τ_c , perfect fluid nature will be developed in quark matter at higher temperature for $B \neq 0$ with respect to its $B = 0$ case. It reflects that for fixed interaction, magnetic field push the system towards KSS bound, while temperature kick away from the bound. To zoom in the fact, we have plotted $\eta_{1,2,3,4}$ vs eB/m_π^2 in Fig. 4, where decreasing trend of $\eta_{1,2}$ with magnetic field is clearly observed. Magnetic field dependent of Hall-type coefficients $\eta_{3,4}$ behave little different because of its anisotropic structure $\frac{(\tau_c/\tau_B)}{1+(\tau_c/\tau_B)^2}$, which increases with B for $\tau_c/\tau_B < 1$ but decreases with B for $\tau_c/\tau_B > 1$. Therefore, we get increasing $\eta_{3,4}(B)$ for $\tau_c = 1$ fm and decreasing $\eta_{3,4}(B)$ for $\tau_c = 20$ fm, as displayed in Fig. 4(b) and (d).

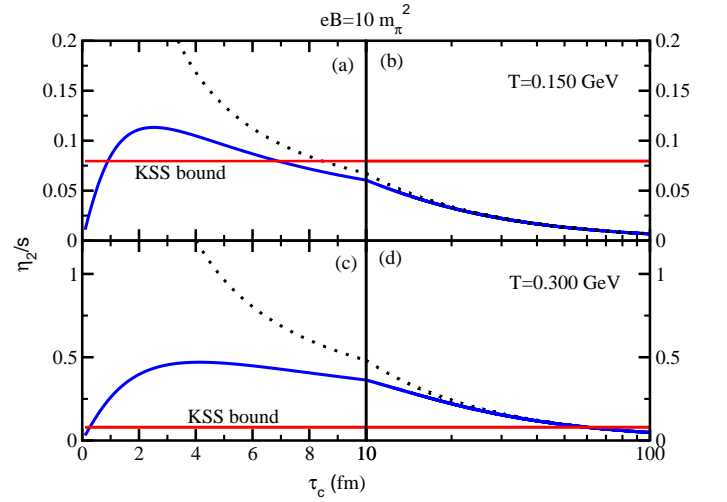


FIG. 5: τ_c dependence of η_2/s from Eq. (32) (solid line) and Eq. (21) (dotted line) at $eB = 10m_\pi^2$, $T = 0.150$ GeV in the range of (a) $\tau_c < 10$ fm and (b) $\tau_c > 10$ fm; and at $T = 0.300$ GeV in the range of (c) $\tau_c < 10$ fm and (d) $\tau_c > 10$ fm. Straight horizontal red line denotes the KSS bound.

Another interesting point has also been shown in Fig. 4. It is regarding the merging of general anisotropic shear viscosity components with their strong field limit estimation. At strong field limit, $\eta_2 = 4\eta_1$ and $\eta_4 = 2\eta_3$, whose expressions are given in Eqs. (21), (22). These strong field limit estimations of $\eta_2 = 4\eta_1$ and $\eta_4 = 2\eta_3$ curves are plotted by dotted line in Fig. 4(a) and (b) respectively for $\tau_c = 1$ fm. On the other hand, general anisotropic components of shear viscosity can be obtained from Eqs. (31), (32), (33), (34) and plotted $4\eta_1$ (red dash line), η_2 (blue solid line), $2\eta_3$ (green dash line), η_4 (orange solid line) in Fig. 4(a) and (b) for $\tau_c = 1$ fm. We notice that these curves are not merging in any point of B -axis up to $eB = 15m_\pi^2$ but when we use $\tau_c = 20$ fm in Figs. 4(c,d), they are merging after $eB = 6m_\pi^2$. It tells that strong field limit might be good approximation for $\tau_c > 10$ fm but for RHIC or LHC matter, whose $\tau_c < 10$ fm, strong field limit expressions might not be considered as a good approximated estimation. This picture will be more clear in Fig. 5, which exposes the τ_c dependence of η_2/s from Eq. (32) (solid line) and Eq. (21) (dotted line) at $eB = 10m_\pi^2$, $T = 0.150$ GeV in the range of (a) $\tau_c < 10$ fm and (b) $\tau_c > 10$ fm. Here, we find how general η_2/s is merging with its strong field limit curves in second zone ($\tau_c > 10$ fm), while they are quite far in first zone ($\tau_c < 10$ fm). Same qualitative pattern is also noticed for $T = 0.300$ GeV in Fig. 5(c,d). From the crossing of KSS line in Fig. 5, we can say that nearly perfect fluid nature can be obtained for two different values of τ_c within $\tau_c < 10$ fm zone at $eB = 10m_\pi^2$, $T = 0.150$ GeV. We can denote them as τ_c^\mp . The values of τ_c^- is seen below 1 fm, so it might not be reached in RHIC or LHC matter. So τ_c^+ is more phenomenological point.

Interestingly, we notice that τ_c^+ remain $\tau_c > 10$ fm zone for $T = 0.300$ GeV. Hence, alternatively we can say that to build nearly perfect fluid nature in higher temperature quark matter, we need higher magnetic field if we want it for $\tau_c < 10$ fm zone. It is quite possible for RHIC or LHC matter, having $\tau_c < 10$ fm zone, where high magnetic field decays with time and temperature. I means that as we approach higher temperature, that matter can face higher magnetic field in experiments. So there might be a compensating role of temperature and magnetic field to build nearly perfect fluid nature in RHIC or LHC matter.

V. SUMMARY

We have studied shear viscosity of quark matter in a uniform magnetic field background, where the medium loses its isotropic property. Due to this anisotropic nature, one can get more than one components of shear viscosity, denoted by η_1, η_2, η_3 and η_4 , which are ultimately reduced to two main components in strong field limit through relations $4\eta_1 = \eta_2$ and $2\eta_3 = \eta_4$. We know that isotropic shear viscosity η in absence of magnetic field is mainly governed by two parts - the phase space and the relaxation time. Here also η_2 and η_4 can be casted into the similar structure with phase space and relaxation time parts. The relaxation time of η_4 is inversely proportional to synchrotron frequency ω_B and relaxation time of η_2 is $\frac{\Gamma_c}{(\omega_B)^2}$ in strong field limit, where collisional thermal width Γ_c of medium constituents will be much smaller than its synchrotron frequency i.e. $\Gamma_c \ll \omega_B$. Although, a large values of Γ_c is expected for strongly-coupled RHIC or LHC matter. To describe that zone, we need a general structure of $\eta_{1,2,3,4}$, which don't follow the relations $4\eta_1 = \eta_2$ and $2\eta_3 = \eta_4$ below the strong field domain.

We have used the formalism of NJL model in presence of magnetic field to describe the magneto-thermodynamics of quark matter and we get a temper-

ature and magnetic field dependent quark mass, which will enter to the phase space factors of $\eta_{1,2,3,4}$. In strong field limits, all components decrease with B but in weak field case, the Hall-type viscosities $\eta_{3,4}$ increase with B .

Along with the constant value τ_c , we have also calculated T dependent of τ_c from simple contact diagram of $2 \rightarrow 2$ scattering processes, coming from the interaction Lagrangian density of NJL model. Replacing T dependent quark mass $M_Q(T)$ by T, eB dependent quark mass $M_Q(T, eB)$, we have extended the expression of relaxation time from $\tau_c(T)$ to $\tau_c(T, eB)$. Scattering probability (Γ_c) proportionally increases with density of medium, which increases with T due to statistical reason and decreases with eB due to mass enhancement. Hence, relaxation time $\tau_c(T, eB)$ decreases with T and increases with eB . In absence of magnetic field, shear viscosity to entropy density ratio decreases with T as it is proportional to relaxation time but it increases with T in strong field picture as it is inversely proportional to the relaxation time. So, transition from without to with magnetic field picture, T dependence of viscosity to entropy density ratio transforms from decreasing to increasing trends.

In present work, we have calculated $\tau_c(T, eB)$ from simplest contact diagram $2 \rightarrow 2$ scattering processes, which provide a large τ_c , where $eB = 10m_\pi^2$ can safely be considered as strong field case. However, to describe RHIC or LHC matter with small τ_c , we have to consider the general structure of $\eta_{1,2,3,4}$ and better interaction picture, which can map strongly-coupled matter. We keep this problem as our future goal, which definitely provide an up-gradation of research on transport properties of quark matter under external magnetic field.

Acknowledgment: SG acknowledges to Indian Institute of Technology (IIT) Bhilai, funded by Ministry of Human Resource Development (MHRD) as well as earlier D. S. Kothari fellowship, University Grants Commission (UGC) under grant No. F.4-2/2006 (BSR)/PH/15-16/0060. SG and AM thank to Pracheta Singha for initial constructive discussion on this work.

-
- [1] T. Schafer, D. Teaney, Rep. Prog. Phys. **72** (2009) 126001.
 - [2] K. Tuchin, Adv. High Energy Phys. **2013** (2013).
 - [3] V. Skokov, A. Y. Illarionov and V. Toneev, Int. J. Mod. Phys. A **24**, 5925 (2009).
 - [4] V. Voronyuk, V. D. Toneev, W. Cassing, E. L. Bratkovskaya, V. P. Konchakovski and S. A. Voloshin, Phys. Rev. C **83**, 054911 (2011).
 - [5] A. Bzdak and V. Skokov, Phys. Lett. B **710**, 171 (2012).
 - [6] W. T. Deng and X. G. Huang, Phys. Rev. C **85**, 044907 (2012).
 - [7] W. T. Deng and X. G. Huang, Phys. Lett. B **742**, 296 (2015).
 - [8] J. O. Andersen, W. R. Naylor and A. Tranberg, Rev. Mod. Phys. **88**, 025001 (2016).
 - [9] V. A. Miransky and I. A. Shovkovy, Phys. Rept. **576**,1 (2015).
 - [10] R. Gatto, M. Ruggieri, Phys. Rev. D **83** (2011) 034016.
 - [11] R. Gatto, M. Ruggieri, Lect.Notes Phys. **871** (2013) 87; arXiv:1207.3190 [hep-ph].
 - [12] J. K. Boomsma and D. Boer, Phys. Rev. D **81**, 074005 (2010).
 - [13] B. Chatterjee, H. Mishra, A. Mishra, Phys. Rev. D **84**, 014016 (2011).
 - [14] B. Chatterjee, H. Mishra, A. Mishra, Phys. Rev. D **91**, 034031 (2015).
 - [15] G. S. Bali, F. Bruckmann, G. Endrodi, Z. Fodor, S. D. Katz, S. Krieg, A. Schafer and K. K. Szabo, J. High Energy Phys. **1202**, 044 (2012).
 - [16] V. G. Bornyakov, P. V. Buividovich, N. Cundy, O. A. Kochetkov and A. Schafer, Phys. Rev. D **90**, 034501 (2014).
 - [17] A. Ayala, M. Loewe, A. Z. Mizher and Zamora, R., Phys.

- Rev.D **90**, 036001 (2014).
- [18] A. Ayala, M. Loewe and R. Zamora, Phys. Rev. D **91**, 016002 (2015)
- [19] R.L.S. Farias, K.P. Gomes, G.I. Krein, M.B. Pinto Phys. Rev. C **90**, 025203 (2014).
- [20] R.L.S. Farias, V.S. Timoteo, S.S. Avancini, M.B. Pinto, G. Krein, Eur. Phys. J. A **53**, 101 (2017).
- [21] G. Basar, D. E. Kharzeev, and V. Skokov, Phys. Rev. Lett. **109**, 202303 (2012),
- [22] S. Li, H-U Yee, arXiv:1707.00795 [hep-ph].
- [23] S. Nam, C-W Kao, Phys. Rev. D **87**, 114003 (2013).
- [24] M. G. Alford, H. Nishimura and A. Sedrakian, Phys. Rev. C **90**, no. 5, 055205 (2014)
- [25] A. N. Tawfik, A. M. Diab, M. T. Hussein, Int. J. Adv. Res. Phys. Sci. 3 (2016) 4.
- [26] K. Tuchin, J. Phys. G: Nucl. Part. Phys. 39 (2012) 025010.
- [27] K. Hattori, X. G. Huang, D. H. Rischke and D. Satow, arXiv:1708.00515 [hep-ph].
- [28] X-G Huang, M. Huang, D. H. Rischke, A. Sedrakian, Phys. Rev. D **81**, 045015 (2010).
- [29] X. G. Huang, A. Sedrakian and D. H. Rischke, Annals Phys. **326**, 3075 (2011)
- [30] P. Mohanty, A. Dash, V. Roy, arXiv:1804.01788 [nucl-th].
- [31] N.O. Agasian, Phys. Atom. Nucl. 76 (2013) 1382.
- [32] N.O. Agasian, JETP Lett. 95 (2012) 171.
- [33] S. i. Nam, Phys. Rev. D **86**, 033014 (2012).
- [34] K. Hattori, D. Satow, Phys. Rev. D **94**, 114032 (2016).
- [35] K. Hattori, S. Li, D. Satow, H.-U. Yee, Phys. Rev. D **95**, 076008 (2017).
- [36] A. Harutyunyan and A. Sedrakian, Phys. Rev. C **94**, no. 2, 025805 (2016).
- [37] B. O. Kerbikov and M. A. Andreichikov, Phys. Rev. D **91**, no. 7, 074010 (2015)
- [38] B. Feng, Phys. Rev. D **96**, 036009 (2017).
- [39] P. V. Buividovich, M. N. Chernodub, D. E. Kharzeev, T. Kalaydzhyan, E. V. Luschevskaya and M. I. Polikarpov, Phys. Rev. Lett. **105**, 132001 (2010).
- [40] K. Fukushima, Y. Hidaka, arXiv:1711.1472 [hep-ph].
- [41] V. Roy, S. Pu, L. Rezzolla and D. Rischke, Phys. Lett. B **750**, 45 (2015)
- [42] S. Pu, V. Roy, L. Rezzolla and D. H. Rischke, Phys. Rev. D **93**, no. 7, 074022 (2016)
- [43] S. K. Das, S. Plumari, S. Chatterjee, J. Alam, F. Scardina and V. Greco, Phys. Lett. B **768**, 260 (2017)
- [44] R. Critelli, S.I. Finazzo, M. Zaniboni, J. Noronha, Phys. Rev. D **90**, 066006 (2014); S. I. Finazzo, R. Critelli, R. Rougemont and J. Noronha, Phys. Rev. D **94**, 054020 (2016).
- [45] S. Jain, R. Samanta, S. P. Trivedi, J. High Energy Phys. 10 (2015) 028.
- [46] M. Frank, M. Buballa and M. Oertel, Phys. Lett. B **562**, 221 (2003).
- [47] S. Gavin, Nucl. Phys. A, **435**, 826 (1985).
- [48] P. Chakraborty and J. I. Kapusta, Phys. Rev. C **83**, 014906 (2011).
- [49] E.M. Lifshitz and L.P. Pitaevskii, 1987 *Physical kinetics*, Pergamon Press, U.K.
- [50] A. Abhishek, H. Mishra , S. Ghosh Phys.Rev. D97 (2018) 014005.
- [51] P. Singha, A. Abhishek, G. Kadam, S. Ghosh, H. Mishra, J. Phys. G **46** (2019) 015201.
- [52] P. Deb, G. P. Kadam, H. Mishra Phys.Rev. D94 (2016) 094002.
- [53] S. Ghosh, T. C. Peixoto, V. Roy, F. E. Serna, G. Krein, Phys. Rev. C **93** (2016) 045205.
- [54] S. Ghosh, F. E. Serna, A. Abhishek, G. Krein, H. Mishra, Phys.Rev. D99 (2019) 014004.